The arising of anisotropy and inhomogeneity in a isotropic viscoelastic model of the passive myocardium

The arising of anisotropy and inhomogeneity in a isotropic viscoelastic model of the passive myocardium.

Richard van Gemert

92.032

Abstract.

The aim of this study is to verify to which extent the experimentally observed difference between fiber and cross fiber stiffness of passive myocardial tissue can be predicted by means of anisotropic loading of a viscoelastic isotropic model. The elastic response is described by a simple strain-energy function which relates the second Piola-Kirchhoff stress with the Green-Lagrange strain. The time dependent component is modelled by means of quasi-linear viscoelasticity. This is implemented into a program which simulates passive deformation of a small cardiac specimen. When enforcing a cyclic fiber and cross-fiber stretch consistent with experimental measurements in the beating heart, this program shows that after 16044 beats, the difference between zero stress fiber stiffness and zero stress cross-fiber stiffness equals 25 % of its value endocardially and 8 % of its value epicardially.

Introduction.

It appears from experimental measurements on biaxial properties of cardiac tissue that myocardial tissue is no linearly viscoelastic (Yin et al., 1987). At the same time the experiments show that the stress-strain curves are different in the direction of the muscle fiber and in their plane cross-fiber direction. Yin et al. (1987) conclude that the tissue is anisotropic elastic and inhomogeneous.
The purpose of this study is to show that by means of a simple biaxial viscoelastic model and an isotropic viscoelastic law, the dependence on the loading direction of the strain-stress curve can be explained. Before I work out the method of modelling, I will give a description of those properties of the cardiac muscle which are of importance to the purpose of this work.

Cardiac muscle.

The cardiac muscle consist of three layers: endo-, myo- and epicardium. Endocardium is the inner layer of the heart wall, consisting of an endothelial lining resting upon connective tissue. Myocardium consists of muscular cells, which form fibers. The fibers unit into bundles which forms a three dimensional net-work . Between this there is also a rich capillary bloedvessels net-work, longitudinal and transverse tubules, collagene bonds between the fibers and physiological

liquid. The difference between the outerwall of the myocardium, the epicard, and the inner wall, the endocard, is shown by the orientation of the fibers in a layer. The muscular cells are striated and are made up of sarcomeres. The basic mechanism of contraction is similar to that of a skeletal muscle. Epicardium is the outer layer of the heart wall, consisting of connective tissue.
Although the cardiac muscle consists of many cells, it behaves as a whole by activation, that's why the cardiac muscle is said to be the semblance of a syncytium. Compared with skeletal muscles, there is an abundance of mitochondria in the cardiac muscle. The cardiac muscle relies on the large number of mitochondria to keep pace with its energy need. The cardiac muscle possesses resting tension in the normal function of the heart which is significant. Because of the resting tension, the operational range of the heart muscle is quite limited (Y. Fung,1981). The resting tension determines the end-diastolic volume and thus the stroke volume of the heart.

Passive cardiac muscle.

Cardiac muscle in resting state is an inhomogeneous and nearly incompressible material. The cardiac properties depend on environmental conditions. The cardiac muscle in resting state is also viscoelastic, because it exhibits stress relaxation, creep and it dissipates energy in cyclic loading and unloading.
Viscoelastic materials have an ill-defined stress free state. This shortage forthcoming, in a experiment specimens of viscoelastic material are preconditioned. So repeatable mechanical responses are obtained to stress and strain. Stress-free states measured before and after preconditioning is generally different. Nevertheless, the effects of preconditioning are not allowed to confound with viscoelastic material properties.
A relaxation test can be done to quantify viscoelastic properties. A quick change in strain is laid on a specimen, which generates a tensile stress. The change in strain should be a step change but this is not practical to establish and it causes stress waves which travel in the specimen so that uniform strain throughout the specimen cannot be obtained.

Active cardiac muscle.

Waldman et al. (1985,1988) measured three dimensional finite strain in the beating canine heart relative to its enddiastolic state. The principal directions of deformation vary little from epicardium to endocardium, despite the fact that myofiber direction varies across the wall and the sarcomeres would be expected to shorten only along their axes (Waldman et al., 1988).
The principal directions of deformation vary substantially

with time during contraction. At end-ejection fiber direction and first principal strain direction of greatest shortening are not substantially different in the outer half, they are virtually orthogonal to each other in the inner half of the wall. Nevertheless, substantial subendocardial shortening deformation along the fiber direction tends to occur during contraction with a magnitude about half its value along the cross fiber direction.

Model.

As said, a viscoelastic isotropic model relates the total second Piola-Kirchhoff stress with the Green-Lagrange strain.

The Green-Lagrange strain is defined as:

$$\varepsilon = 0.5 \cdot \left(\left(\frac{L}{L_0} \right)^2 - 1 \right)$$

The total second Piola-Kirchhoff stress (Huyghe, 1986) is equal to

$$S^t_{if}(\varepsilon_{cf}(t), \varepsilon_{ff}(t), t) = S^e_{if}(\varepsilon_{cf}(t), \varepsilon_{ff}(t)) + S^v_{if}(\varepsilon_{cf}(t), \varepsilon_{ff}(t), t)$$

with S^t_{if}= total stress

S^e_{if}= elastic stress

S^v_{if}= viscoelastic stress

ε_{cf}= strain in cross-fiber direction
ε_{ff}= strain in fiber direction
i = c,f.

The elastic response of the passive cardiac muscle will be described by a simple strain-energy function W:

$$W(\varepsilon_{ff}(t), \varepsilon_{cf}(t)) = c * \exp\left(a * \left((\varepsilon_{ff}(t))^2 + (\varepsilon_{cf}(t))^2 \right)\right)$$

with a= exponential stiffness
c= initial stiffness.

This function is a simplified two dimensional version of the strain-energy function of Bovendeerd (1990).
The material parameters a and c are adjusted so that the experimental results of uniaxial stretch obtained from Ter Keurs (1990) are approximated (appendix A). Because the stress

free state is ill-defined, the parameters a and c are different after a new computation. The strain changes for the stress free state, so to satisfy the results of Ter Keurs the parameters a and c are adjusted. New computations are done till the initial strain is reached and the stress free state is well defined.

From the strain-energy function the elastic second Piola-Kirchhoff stress can be derived,

$$S^{e}_{if}(\varepsilon_{cf}(t),\varepsilon_{ff}(t)) = \partial W(\varepsilon_{cf}(t),\varepsilon_{ff}(t)) / \partial \varepsilon_{if}(t)$$

with i= c,f.

The expression for the viscoelastic second Piola-Kirchhoff stress is:

$$S^{v}_{if}(\varepsilon_{cf}(t),\varepsilon_{ff}(t),t) = \int_{-\infty}^{t} \frac{d}{d\tau} G(t-\tau)\, S^{e}(\varepsilon_{cf}(\tau),\varepsilon_{ff}(t))\, d\tau$$

with G(t)= reduced relaxation function
i= c,f.

Implementation of this expression in a numerical program is tendentious because all this can be formulated as a recurrent relationship (appendix B).

The reduced relaxation function G(t) is of the form

$$G(t) = \frac{[1 + \int_{0}^{\infty} S(\tau)\, e^{-\frac{t}{\tau}} d\tau]}{[1 + \int_{0}^{\infty} S(\tau)\, d\tau]}$$

$S(\tau)= d/\tau, \quad \tau_1 \leq \tau \leq \tau_2$

$S(\tau)= 0$ elsewhere
d= damping constant.

A numerical better expression of this function is also given in appendix B.
Because the passive cardiac muscle is a mixture, in the reduced relaxation the generalized Maxwell model is used. This model describe a viscoelastic mixture well and it approximates the cardiac muscle also well.

The total Cauchy stress is known. Now a strain in cross-fiber and fiber direction is imposed. In recollection, viscoelastic material have not a well-defined stress free state. So the stress free state is estimated. For the cross-fiber direction this is in the endocardial equator 0.035 and for the epicardial equator 0.03. For the fiber direction this is in the endocardial equator 0.06 and for the epicardial equator the strain is 0.025. The derivation from epicardial strains is found in appendix C, the derivation is obtained from the data of Andrew et al.(1989). The endocardial stains are obtained from computation results from J. Huyghe (1986).
To simulate systolic and diastolic strains the data from Waldman et al. (1988) is used. In cross-fiber direction this is endocardially 0.085, epicardially 0.02 and in fiber direction this will be endocardially 0.03 and epicardially 0.045. These data also have relations with the equatorial free wall. This is half between the apex and the bases. The choice for the equator is not random. This is choosen because data is easy got from the equator.

The last step that has to be done is to compute the instantaneous stiffness. This can be derived from

$$\partial S^{t}_{if}(\varepsilon_{cf}(t),\varepsilon_{ff}(t),t)/\partial\varepsilon_{if}(t)$$

This partial derivative is approximated by

$$\frac{S^{t}_{if}(\varepsilon_{cf}(t)+0.01,\varepsilon_{ff}(t)+0.01)-S^{t}_{if}(\varepsilon_{cf}(t),\varepsilon_{ff}(t))}{0.01}$$

which is allowed because (see appendix D)

$$S^{v}_{if}(t_{n+1})-S^{v}_{if}(t_{n}) \qquad if \quad t_{n+1}\rightarrow t_{n}$$

The instantaneous stiffness is computed after n strain cycli are imposed. In order to approximate the reality the total stress will not go at once to zero but it will go to zero in 20 time-steps.

Results.

To show that the passive cardiac muscle is viscoelastic figure 1 is added. Figure 1 shows hysteresis loops and it shows also a shift in the stress-strain relation. It is caused by viscoelastic properties.

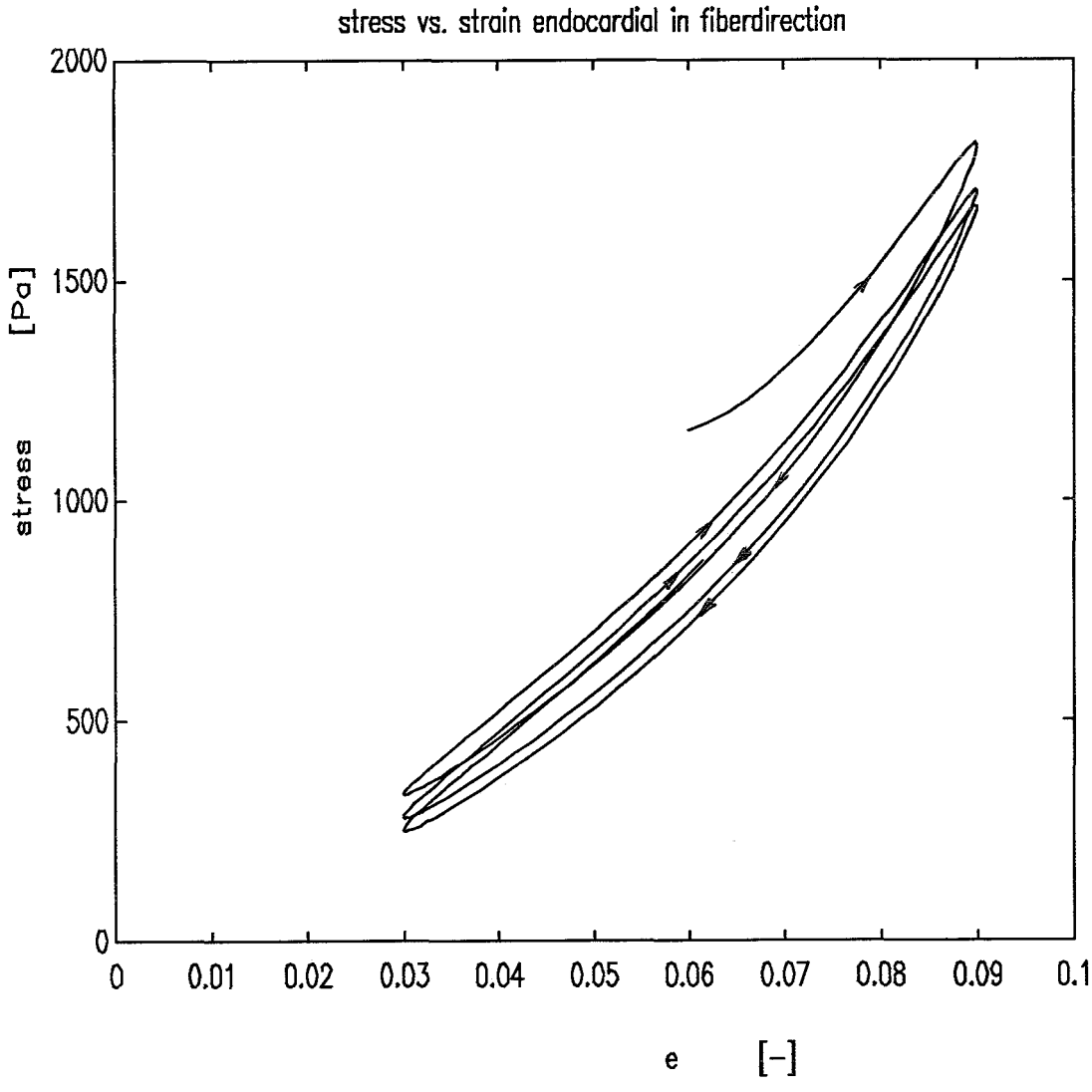

FIGURE 1: shows that energy is dissipated in cyclic loading and unloading loops and it illustrates a shift in magnitude when more loops are made.

In figure 2 the values of the relaxation function used in this work are plotted. The values for figure 2 are obtained from the data of Lundin (1944). These data are old, but Lundin is the only one who describes a relaxation test longer than two hours. After four hours (τ^2= 14400 sec) the relaxation is 80% of the initial stress value.
As τ^1= 0.01 sec then the value of the damping constant can be derived, d= 0.28 (Pinto et al., 1980).

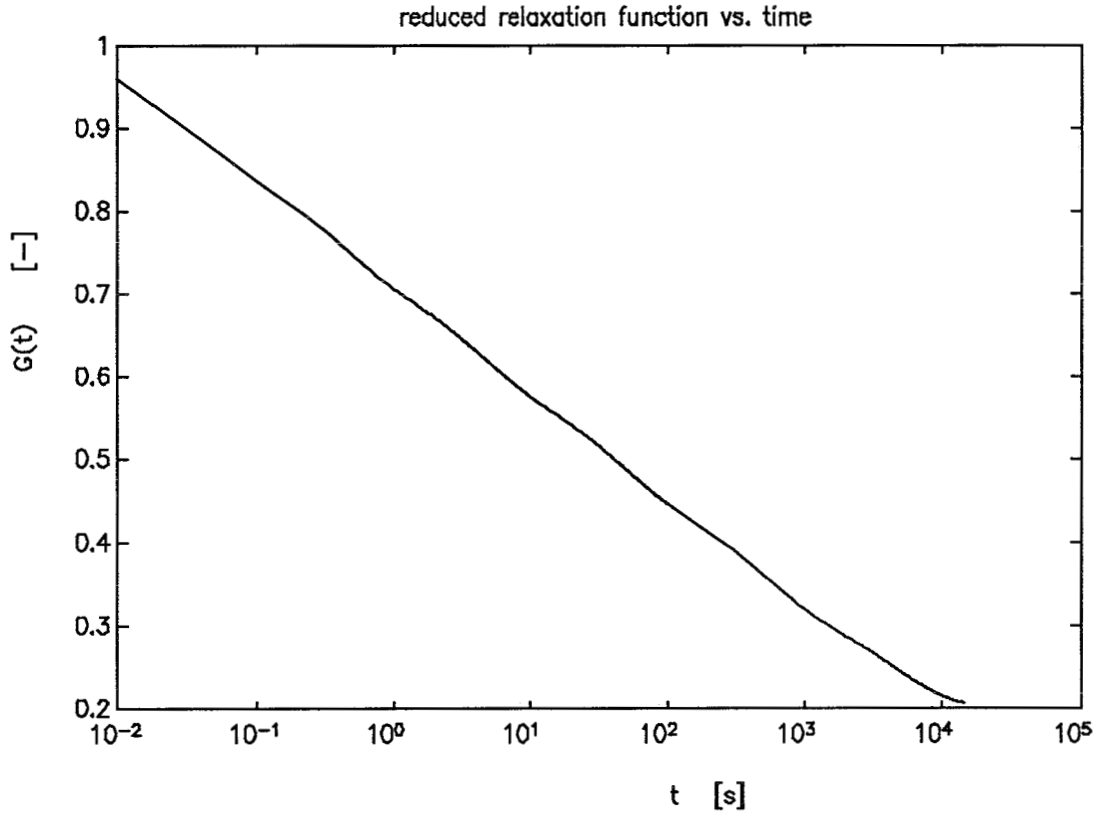

FIGURE 2:The reduced relaxation function with τ^1=0.01 sec, τ^2=14400 sec and d=0.282.

As seen, at the specimen ε_{ff} and ε_{cf} are imposed. This lasts till relaxation time τ^2. Then the stress goes to zero in twenty steps. On account of viscoelasticity there will be residual strains in the specimen. A new computation is done using initial strains equal to the sum of the computed residual strains and the initial strains. The above has to been repeated until the net strain difference between the initial strain and the residual strain equals the experimentally measured value. When this is reached, than the initial strain is chosen well. This is not completely reached in this study (see note in appendix E). It is seen that the epicardial and endocardial wall have different material parameters (appendix E).
To show that anisotropy arises the same linearly increasing stretch in fiber and cross-fiber directions are imposed immediately after the stress becomes zero. The computed residual strain is considered as the initial strain. Results are shown in figure 3 and 4. A difference between the stress in fiber and cross-fiber direction is observed (this is anisotropy).

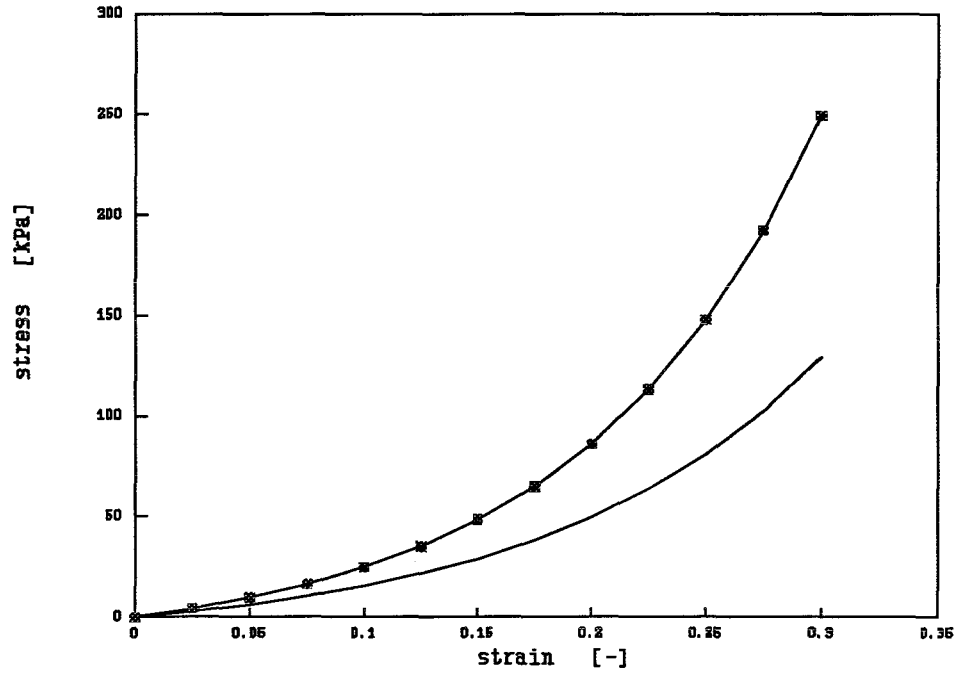

FIGURE 3: Stress versus strain curves in fiber and cross-fiber direction of the endocardial layers are shown. The curve with symbol is svs-curve in ff-direction.

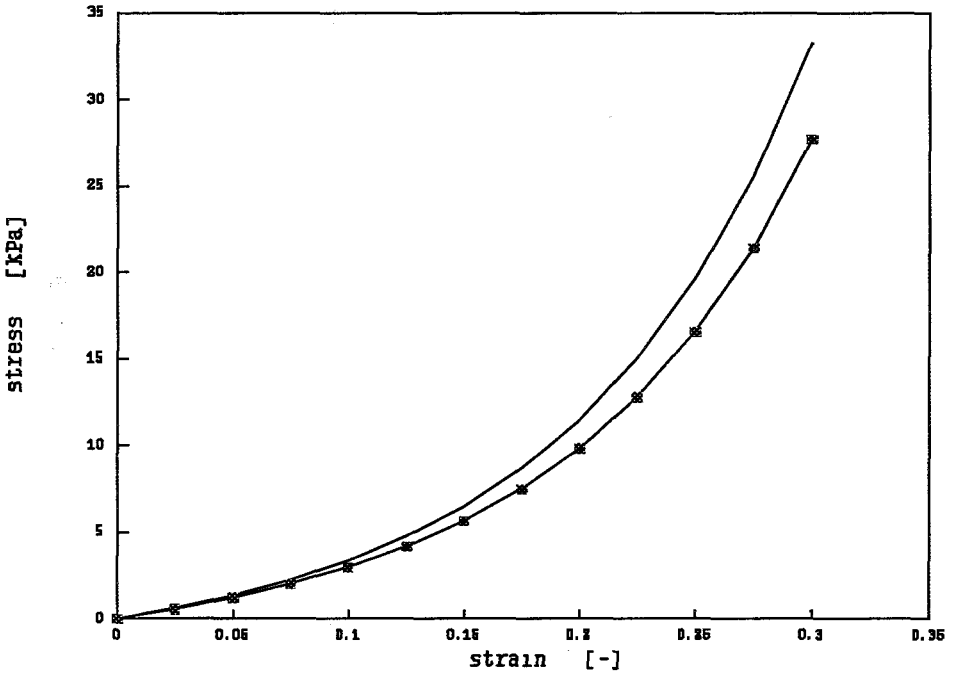

FIGURE 4: Stress versus strain curves in fiber and cross-fiber direction of the epicardial layers are shown. The curve with symbol is the svs-curve in ff-direction. The magnitude of anisotropy is smaller than the magnitude of endocardial anisotropy and in ff-direction the stress is smaller than in cf-direction, which is the reversed of the endocardial situation.

Cardiac muscle has the following property,

$$\frac{instant \cdot stiffn \cdot_{ffend}}{instant \cdot stiffn \cdot_{cfend}} > \frac{instant \cdot stiffn \cdot_{ffepi}}{instant \cdot stiffn \cdot_{cfepi}}$$

The results of the tests meet this.

Discussion.

This study shows that (1) the observed difference between fiber and cross-fiber stiffness of myocardial tissue can be derived from an isotropic viscoelastic material law, (2) regional variations of the fiber and cross-fiber stiffness ratio may result from regional variations in fiber and cross-fiber strain history.

Accuracy.

Discretization of the continuous spectrum has an influence upon the accuracy. However Maessen (1983) shows that the accuracy increases fast when the number of Maxwell elements increases. The greater the difference between relaxation times, the more Maxwell elements are needed to get a better accuracy. In the program 6 Maxwell elements are used, which correspond with a high accuracy. The magnitude of the time step also affects the accuracy. The smaller the magnitude,the greater the accuracy. But the CPU-time increases when the magnitude decreases. After some tests it appears that a time step of 0.01 sec has a deviation of one promille compared with a time step of 0.001 sec. So, a time step of 0.01 sec has been chosen.

Strain.

As noticed before,the magnitude of the initial strain has a great influence upon the final result. This can be seen when the initial strains of the previous tests are studied well. The difference between the epicardial strains is smaller than the difference between the endocardial strains. Anisotropy arises most clearly at the endocardial layers. Tests have shown that the larger the difference the better anisotropy arises. One thing is clear. There is a difference in initial strain and in passive strain, so anisotropic will arise always but the magnitude can vary.

Reality.

The model is simple and two dimensional. Strain is imposed in a constant direction. In reality the direction of the strain varies, the geometric is complex and three dimensional. In reality there are shear stresses and the heart structure will change. The data include different animals, which is not ideal. Futher research should elucidate the influence of these factors on the simulation results.

Conclusion.

The simple biaxial viscoelastic and isotropic model shows that anisotropic of tangent stiffness and inhomogeneity arised. This means that Yin's experiments do not show conclusively that myocardial tissue is intrinsically anisotropic and inhomogeneous .

I wish to thank Dr.Ir. J.Huyghe for his great support and patience.

Richard van Gemert,
January 1992.

References.

Bovendeerd, P.H. The mechanics of the normal and ischemic left ventricle during the cardiac cycle. PhD thesis, Univ. of Maastricht, The Netherlands, 16-68, 1990.

Fung, Y.C. Biomechanics: mechanical properties of living tissues. Springer-Verlag, New York, ch.7 and ch.10 ,1981.

Huyghe, J.M. Non-linear finite element models of the beating left ventricle and the intramyocardial coronary circulation. PhD thesis, Eindhoven Univ. of Technology , Eindhoven, The Netherlands, 3.27-3.32 1986.

Lundin, G. Mechanical properties of cardiac muscle. Acta physiologica Scandinavica vol. 7. supplementum XX, 61-69, 1944.

McCulloch A.D. et al. Regional left ventricular epicardial deformation in the passive dog heart. Circulation research, vol.64, no.4, 1989.

Meassen, P. De berekening van spanningen en vervormingen in snelhardende komposiet materialen. MS thesis, Eindhoven Univ. of Technology WFW, Eindhoven, The Netherlands, 58-63, 1983.

Pinto, J.G. et al. Visco-elasticity ofpassive cardiac muscle. Journal of Biomechanical Enginieering, vol.102, 57-61, 1980.

Ter Keurs et al. Tension development and sacromere length in rat cardiac trabeculae: evidence of length-dependent activation. Circulation research, vol.47, 703-714, 1990.

Waldman et al. Transmural myocardial deformation in the canine left ventricle. Circulation research, vol.57, no.1, 1985.

Waldman et al. Relation between transmural deformation and local myofiber direction in canine left ventricle. Circulation research, vol.63, no.3, 1988.

Yin, F.C. et al. Quantification of the mechanical properties of noncontracting canine myocardium under simultaneous biaxial loading. J.Biomechanics, vol.20, no.6, 1987.

Appendix A

Calculation of the material parameters a and c.

In the following figure the results of uniaxial stretch experiments in 20 rat trabeculae is given [Ter Keurs et al.,1990]. Passive stress is plotted versus sarcomere length l_s. Sarcomere length in the unloaded state equals 1.85 μm.

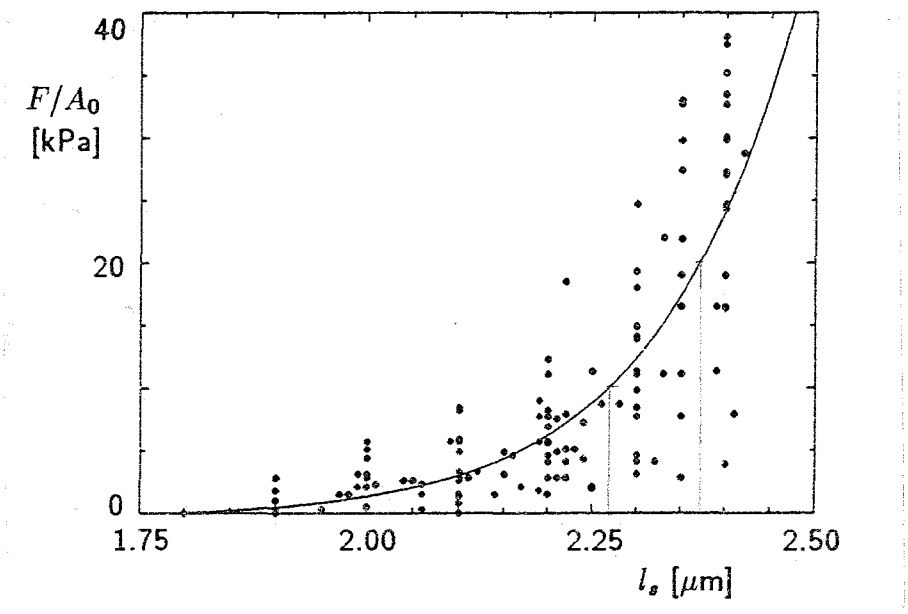

The Green-Lagrange strain is given by

$$E=\frac{1}{2}\left(\left(\frac{l}{l_0}\right)^2-1\right)$$

At sarcomere length 2.268 μm the passive stress is 10 kPa.
At sarcomere length 2.368 μm the passive stress is 20 kPa.

So the strain is 0.251 respectively 0.319.

Thus the following two equations can be drafted

$$1*10^4=2\cdot a\cdot c\cdot 0.251\cdot e^{a\cdot(0.251)^2}$$

$$2*10^4=2\cdot a\cdot c\cdot 0.319\cdot e^{a\cdot(0.319)^2}$$

The solutions of these equations are a=11.7 and c=814.7 kPa.

Appendix B

Before the recurrent relationship of the viscoelastic cauchy stress relation is given, a numerical better expression of the reduced relaxation function is derived.

The reduced relaxation function.

The reduced relaxation function is given by

$$G(t) = \frac{[1 + \int_0^\infty \frac{d}{\tau} e^{-\frac{t}{\tau}} d\tau]}{[1 + \int_0^\infty \frac{d}{\tau} d\tau]}$$

The continuous spectrum $S(\tau)$ can be discretized in m Maxwell elements,

$$\int_0^\infty \frac{d}{\tau} e^{-\frac{t}{\tau}} d\tau = \sum_{j=1}^{m} \int_{\tau(j-1)}^{\tau(j)} \frac{d}{\tau} e^{-\frac{t}{\tau}} d\tau \cong \sum_{j=1}^{m} \frac{d \ln \frac{\tau^2}{\tau^1}}{m} e^{-\frac{t}{\tau\tau(j)}}$$

where:

$$\tau\tau(j) = \tau^1 e^{\frac{j-\frac{1}{2}}{m} \ln \frac{\tau^2}{\tau^1}}$$

with i= c, f
j= 1, m.

Thus

$$G(t) \cong G^{(m)}(t) = \frac{1 + \frac{d \ln \frac{\tau^2}{\tau^1}}{m} \sum_{j=1}^{m} e^{-\frac{t}{\tau\tau(j)}}}{1 + d \ln \frac{\tau^2}{\tau^1}}$$

Recurrent relationship of the viscoelastic stress.

As seen the expression of the viscoelastic stress is equal to

$$S^v(\varepsilon_{if}(t),t)=\int_{-\infty}^{t}\frac{d}{d\tau}G(t-\tau)\,S^e(\varepsilon_{if}(\tau))\,d\tau$$

Partial integration yields

$$S^v{}_j(\varepsilon_{if}(t),t)=\int_0^{t}\frac{d\ln\frac{\tau^2}{\tau^1}}{\tau\tau(j)\cdot(1+d\ln\frac{\tau^2}{\tau^1})}e^{-\frac{\tau}{\tau\tau(j)}}S^e(\varepsilon_{if}(t-\tau))\,d\tau$$

with i= c, f
j= 1, m.

The viscous stresses S^v_j at time $t_{n+1} = t_n+\Delta t_{n+1}$ can be derived from the viscous stresses at time t_n and the previous intergration with substitution from $\tau' = \tau - \Delta t_{n+1}$, thus

$$S^v{}_j(\varepsilon_{if}(t_{n+1}),t_{n+1})=e^{-\Delta\frac{t_{n+1}}{\tau\tau(j)}}[S^v(\varepsilon_{if}(t_n),t_n)+\int_{-\Delta t_{n+1}}^{0}\frac{(d\ln(\frac{\tau^2}{\tau^1}))/m}{1+d\ln\frac{\tau^2}{\tau^1}}e^{\frac{-\Delta t_{n+1}}{\tau\tau(j)}}S^e(\varepsilon_{if}(t_n-\tau')\,d\tau']$$

If the elastic response is assumed to vary linearly within the time step then

$$S^v{}_j(\varepsilon_{if}(t_{n+1}),t_{n+1})=e^{\frac{-\Delta t_{n+1}}{\tau\tau(j)}}S^v(\varepsilon_{if}(t_n),t_n)+\frac{(d\ln\frac{\tau^2}{\tau^1})/m}{1+d\ln\frac{\tau^2}{\tau^1}}\cdot$$

$$[S^e(\varepsilon_{if}(t_{n+1}))-S^e(\varepsilon_{if}(t_n))\,e^{\frac{-\Delta t_{n+1}}{\tau\tau(j)}}$$

$$-\frac{\tau\tau(j)}{\Delta t_{n+1}}(1-e^{\frac{-\Delta t_{n+1}}{\tau\tau(j)}})(S^e(\varepsilon_{if}(t_{n+1}))-$$

$$S^e(\varepsilon_{if}(t_n))]$$

This equation is implemented in the program.

Appendix C

The end diastolic pressure is required from Waldman et al. (1988) and is about 4.7 mm Hg.
This means a volume change of about 16 ml in the left ventricular, see the following figure (Mc.Culloch. et al, 1989).

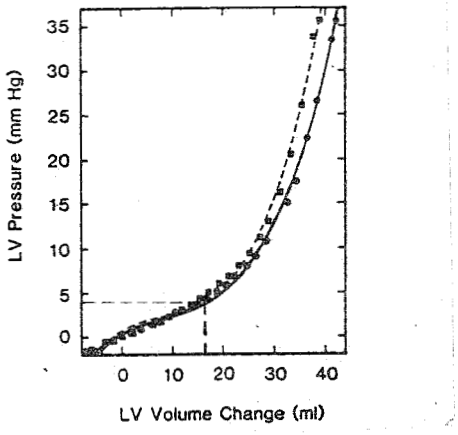

It also follows from Mc.Culloch that the principal extension in fiber direction is 7% and in cross-fiber direction is 5%, epicardial, see the following figure.

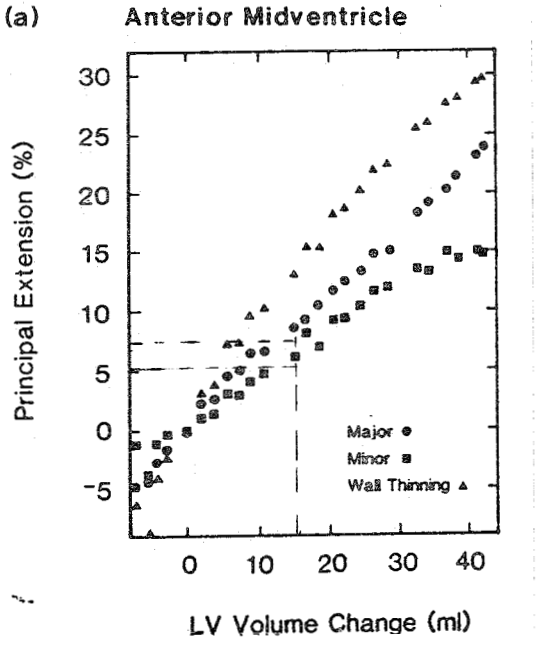

Endocardial extensions is picked from the study of J.Huyghe (1986).

Appendix D

In this appendix is proved that

$$S^{v}_{if}(t_{n+1}) - S^{v}_{if}(t_n)$$

which means that calculation of $S^{t}_{if}(\varepsilon_{if}(t)+0.01)$ is independent of time. The numerical advantage of this is that a new beat can calculated without any influence about the viscoelasticity.

Proof:

$$\lim_{\Delta t_{n+1}\to 0} e^{-\frac{\Delta t_{n+1}}{\tau\tau(i)}} - 1 \qquad (1)$$

$$\lim_{\Delta t_{n+1}\to 0} \frac{\tau\tau(i)}{\Delta t_{n+1}}\left(1 - e^{-\frac{\Delta t_{n+1}}{\tau\tau(i)}}\right) - \lim_{\Delta t_{n+1}\to 0} \frac{e^{-\frac{\Delta t_{n+1}}{\tau\tau(i)}}}{1} - 1 \qquad (2)$$

$$S^{v}_{if}(t_{n+1}) - e^{-\frac{\Delta t_{n+1}}{\tau\tau(i)}} S^{v}_{if}(t_n) + Y_i[\, S^{e}(t_{n+1}) -$$

$$S^{e}(t_n)\, e^{-\frac{\Delta t_{n+1}}{\tau\tau(i)}} - \frac{\tau\tau(i)}{\Delta t_{n+1}} \cdot$$

$$(S^{e}(t_{n+1}) - S^{e}(t_n))\left(1 - e^{-\frac{\Delta t_{n+1}}{\tau\tau(i)}}\right)] \qquad (3)$$

Thus substituting (1) and (2) into (3) with the time difference going to zero gives

$$S^{v}_{if}(t_{n+1}) - S^{v}_{if}(t_n)$$

Appendix E

The value of the relaxation function G(14400)= 0.2063.

In the following tables results are given of the material parameters, the residual strain and the ratio between stifness in fiber- and cross-fiber direction.
Table 1 contains the results epicardial, table 2 contains the results endocardial.

A	B	C	D	E	F
1	807.1	11.77	0.01833	0.02276	0.99
5	709.41	9.8	0.00950	0.01113	0.97
10	616.26	8.91	0.00619	0.00698	0.95
15	550.79	8.4	0.00491	0.00544	0.94
20	499.04	8.03	0.00433	0.00475	0.93
25	454.62	7.73	0.00408	0.00442	0.93
29	422.27	7.53	0.00401	0.00432	0.93
G			0.4%	0.4%	7%

Table 1

A	B	C	D	E	F
1	807.1	11.77	0.04849	0.02852	1.04
5	463.93	7.80	0.03419	0.02395	1.22
10	209.97	6.09	0.03322	0.02558	1.29
15	91.699	5.02	0.03451	0.0280	1.29
20	38.691	4.25	0.03585	0.03013	1.28
25	16.082	3.66	0.03691	0.03177	1.26
29	7.7921	3.29	0.03760	0.03286	1.25
G			4%	3%	25%

Table 2

* note: in table 2 the residual strains are not going to zero. This is probably caused by the fact that the imposed strains are of such high that non-linearities play an unpredictable rule.

with in,
column A: the value of the repetition number
column B: the initial stiffness parameter [kPa]
column C: the exponential parameter [-]
column D: the residual strain in fiber direction
column E: the residual strain in cross-fiber direction
column F: the ratio between stiffness fdir. and cfdir.
row G: the choosen end-values of column D, E and F.